This paper appeared in *Proceedings of the 1998 IEEE Conference on Image Processing,* Vol. 1, pp. 587-591, Chicago, IL, October 1998.

A STATISTICAL METHOD FOR DISCRIMINATION OF NATURAL TERRAIN TYPES FROM SAR DATA *

Müjdat Çetin and William C. Karl

Multi-Dimensional Signal Processing Laboratory, Dept. of ECE
Boston University, 8 Saint Mary's Street, Boston, MA 02215, USA

ABSTRACT

In this paper we propose a method for discrimination of underlying textural structures from spotlight-mode synthetic aperture radar (SAR) returns by using a tomographic data acquisition model as the basis for statistical reasoning. We model the hypothesized textures by statistically self-similar processes and formulate the problem in a hypothesis testing framework in the SAR range profile domain without any image formation. We achieve a near-optimal, computationally efficient evaluation of the likelihood test by transforming the data into the multiscale domain.

1. INTRODUCTION

A critical element of various SAR tasks, such as recognition of man-made objects in background clutter or classification of natural terrain types is to reason about the underlying structures based on their textural properties. Traditionally, such statistical inference is performed on the formed imagery [1, 2]. But image formation is not necessarily required in some problems e.g. in discrimination tasks and, in addition to adding potentially unnecessary computation, may actually introduce undesirable artifacts into the formed image, which must then be compensated for in subsequent processing steps. We examine the use of a tomographic data model as the basis for direct statistical inference based on the radar returns rather than on the formed image. We assume a spotlight-mode SAR sensor on an airborne platform, designed for imaging a relatively small ground patch, and construct a likelihood-based discriminator based on range profiles obtained from phase histories.

Our interest is in discrimination, for simplicity we focus on discriminating different terrain types with homogeneous textural structures here. SAR images of two such natural terrain classes are shown in Figure 1.

*This work was supported by the Air Force Office of Scientific Research under Grant F49620-96-1-0028, the National Institutes of Health under Grant NINDS 1 R01 NS34189, and the Army Research Office under Grant ARO DAAG55-97-1-0013.

We model the underlying textures by fractal random fields. Fractal-based descriptions of image texture have previously been used to characterize natural visual imagery [3], and SAR imagery [4]. We carry this characterization into the projectional data domain where we build a likelihood-based discriminator. This discriminator however is not computationally efficient. We transform the range profile magnitude data into the multiscale domain, where we achieve efficient processing by approximate evaluation of the likelihoods. Our method is in the lines of a previous work [5] in discrimination of fractal fields from tomographic data. We essentially extend that approach to the SAR problem, and demonstrate its use on natural scenes. Since our approach does not require image formation, we do not have to collect full-aperture data for a decision. Our aim here is to achieve the probability of detection versus false alarm performance of an image domain discriminator, but use much less data than that collected from the full aperture. We also demonstrate the potential of our approach to be used as a sequential test, running in parallel with data collection.

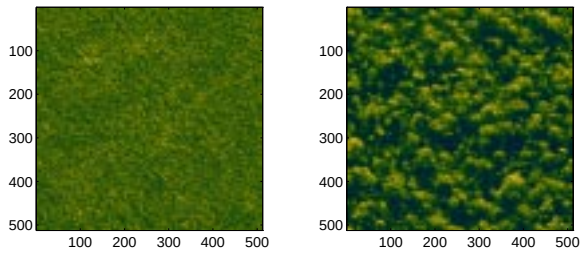

Figure 1: SAR images of natural terrain. Left: grass. Right: forest.

2. SPOTLIGHT-MODE SAR OBSERVATION MODEL

Spotlight-mode SAR data are collected by a radar traversing a flight path and continuously pointing in the direction of a ground patch. At each point corresponding to equal angular increments, high-bandwidth

pulses are transmitted and returns from the ground patch are then received and processed. We will make the typical assumption that linear FM chirp signals are transmitted by the radar. After some preprocessing and certain approximations, the phase history return from a circular patch of radius r at the kth transmission point is given by [6]

$$Z_k(t) = \int_{-r}^{r} p_k(s) exp\left\{-j\frac{2}{c}(w_0 + 2\alpha(t - \frac{2R_0}{c}))s\right\} ds \tag{1}$$

where t denotes time, R_0 is the instantaneous range to the patch center, s is the difference between the instantaneous range to a point in the scene and R_0, c is the speed of light, w_0 is the radar FM chirp carrier frequency, 2α is the chirp rate, and $p_k(s)$ is the sum of complex reflectivities of all points that are equidistant from the radar at a particular transmission point. Thus the observations $Z_k(t)$ are intimately related to the projections $p_k(s) = (\mathcal{T}_k f)(u, v)$ of the underlying field $f(u, v)$. Here $\mathcal{T}_k$ is a projection operator. Now, taking into account the observation kernel in (1) and the projection operation, we can write the following sampled data relationship after appropriate discretization

$$\underbrace{\begin{bmatrix} Z_1 \\ Z_2 \\ \vdots \\ Z_N \end{bmatrix}}_{Z} = \underbrace{\begin{bmatrix} C_1 \\ C_2 \\ \vdots \\ C_N \end{bmatrix}}_{C} f \tag{2}$$

where N is the total number of observation points, f is the underlying sampled reflectivity field column stacked as a vector, Z_k are the discrete versions of the data in (1) and C_k are the discrete observation kernels relating the underlying field to radar returns. Note that since (1) is a band-limited Fourier transform of the projections in the spatial variable s, the data Z are in the (spatial) frequency domain. We can also obtain a spatial domain relationship by defining $z = F^{-1}Z$. Here F is the matrix performing a DFT on each radar return. We can now write the following projectional data relationship

$$z = Tf \tag{3}$$

where $T = F^{-1}C$ represents a discrete "SAR projection operator". Now the problem is to reason about f based on the phase histories Z, or range profiles z. In the following sections we will be focusing on range profile data only.

3. FRACTAL TEXTURE MODELS

We model each natural terrain type by a $1/f$ fractal field of a particular fractal dimension. The measured power spectral density (PSD) $S_f(\omega_u, \omega_v)$ of a $1/f$ fractal field f has the following form [7] :

$$S_f(\omega_u, \omega_v) = \frac{\sigma_f^2}{|\omega|^\gamma} \tag{4}$$

where ω is the angular frequency, σ_f^2 is a constant, and γ is the spectral parameter.

We consider the simplest examples of $1/f$ processes, namely *fractional Brownian motions* (fBms). In fact, since fBm is a nonstationary random process, its PSD is formally undefined; however Flandrin [8] has developed an analytical framework for the generalized PSD of fBm. For any such process, $f(u, v)$ has Gaussian increments with mean zero, and a variance that depends only on the distance between the increments, i.e. $f(u_1, v_1) - f(u_2, v_2) \sim \mathcal{N}(0, \Sigma_{inc})$ where

$$\Sigma_{inc} \propto ((u_1 - u_2)^2 + (v_1 - v_2)^2)^H, \tag{5}$$

and H is the so-called Hurst parameter, with $0 < H < 1$. It is also true that $\gamma = 2H + 2$. The *fractal dimension* D which is commonly used to capture textural differences between fractal fields, is defined as $D = 3 - H$.

In Figure 2, covariance matrices for real-valued fractal fields with different spectral parameters (hence different fractal dimensions) are illustrated. Note that the covariance matrix on the right, corresponding to a larger spectral parameter has wider bands, and a larger number of significant bands which are implications of longer range correlation in the fractal field in the vertical and horizontal directions. Sample fractal fields with these covariance structures are shown in Figure 3. Note that the left field in the figure has a more noise-like behavior (like grass), while the longer range correlation structure is obvious in the right one (like forest). We model the magnitudes of the terrain reflectivities with fractal fields of a certain fractal dimension.

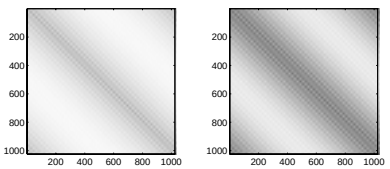

Figure 2: The grayscale plot (black: maximum, white: minimum) of the covariance matrices for the fractal fields. Left: $\gamma = 2$. Right: $\gamma = 3$. The matrices are 1024×1024, since the fields are 32×32.

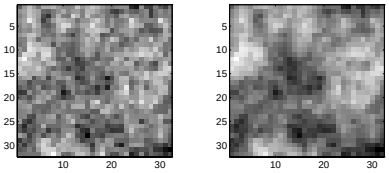

Figure 3: Realizations of 32×32 fractal fields. Left: $\gamma = 2$. Right: $\gamma = 3$.

4. THE DISCRIMINATION PROBLEM

We now formulate the binary discrimination problem in a hypothesis testing framework in the data domain. Let f_i be the complex-valued underlying field corresponding to the ith terrain hypothesis. We will model f_i with a uniform, spatially uncorrelated phase, and a fractal magnitude with covariance Σ_i, where Σ_i corresponds to a particular spectral parameter γ_i. Under the two hypotheses, the noisy range profile observations y are given by

$$H_0 : y = Tf_0 + n \quad H_1 : y = Tf_1 + n \tag{6}$$

where the noise n is uncorrelated with the fields and its real and imaginary parts are distributed as $\mathcal{N}(0, \sigma^2 I)$.

We aim to discriminate the terrain types based on the difference in their fractal correlation structure. However due to the uniform phase property of the underlying fields, the real and imaginary parts of the complex range profiles, which are projectional observations of the field, cannot be discriminated based on their second order properties, i.e. correlation structure. The magnitudes of the range profiles however still carry the fractal properties of the underlying textures. For that reason, we will construct a likelihood-based discriminator in terms of the observed range profile magnitudes $\tilde{y}$. In this discriminator we will need the covariance matrix $\Sigma_{\tilde{y}|f_i}$ of the magnitude data. The uniform phase structure of the fields and the non-linear transformation in obtaining the range profile magnitudes however prevents us from obtaining this matrix exactly in terms of the fractal field covariance matrices Σ_i. So we use an approximate magnitude data covariance matrix $\hat{\Sigma}_{\tilde{y}|f_i} = |T\Sigma_i T^* + 2\sigma^2 I|$, where "$*$" denotes complex conjugate transpose. We form a log-likelihood function $L(\gamma_i)$ corresponding to hypothesis H_i satisfying

$$L(\gamma_i) \propto -ln(|\hat{\Sigma}_{\tilde{y}|f_i}|) - (\tilde{y} - \mu_{\tilde{y}|f_i})^T \hat{\Sigma}^{-1}_{\tilde{y}|f_i} (\tilde{y} - \mu_{\tilde{y}|f_i}) \tag{7}$$

where $\mu_{\tilde{y}|f_i}$ is the mean of the magnitude data. The log-likelihood decision rule for discriminating between the two fields is given by:

$$L(\gamma_1) - L(\gamma_0) \underset{\gamma_0}{\overset{\gamma_1}{\gtrless}} \delta \tag{8}$$

where δ is a threshold parameter that controls the tradeoff between the probability of detection and the probability of false alarm.

5. MULTISCALE DISCRIMINATION OF SAR TEXTURES

The likelihood test described above requires the determinant and inverse of large and full covariance matrices. This is illustrated by the sparsity pattern of a typical range profile magnitude model covariance matrix $\hat{\Sigma}_{\tilde{y}|f_i}$ in the left half of Figure 4. In this figure, elements with magnitudes larger than 1% of the maximum value in the matrix are shown. The existence of many such elements in the covariance matrix makes computation of the determinant and inverse difficult, and hence direct computation of the likelihoods inappropriate. Alternatively, we propose transforming the range profile magnitudes corresponding to each radar return into the multiscale domain by a 1-dimensional Wavelet transform. To this end, let W be a matrix whose blocks perform such a transform on each range profile. Then the multiscale noisy data are given by $\nu = W\tilde{y}$. The log-likelihoods in the multiscale domain obey:

$$L_{ms}(\gamma_i) \propto -ln(|\hat{\Sigma}_{\nu|f_i}|) - (\nu - \mu_{\nu|f_i})^T \hat{\Sigma}^{-1}_{\nu|f_i} (\nu - \mu_{\nu|f_i}). \tag{9}$$

The sparsity pattern of the multiscale data model covariance matrix, $\hat{\Sigma}_{\nu|f_i} = W\hat{\Sigma}_{\tilde{y}|f_i}W^T$ (using the Daubechies wavelet D_{10}, and after ordering the elements in ν from coarse to fine scales) is shown in the right half of Figure 4. Clearly, this matrix is much sparser than the original data model covariance matrix, which suggests an approximate likelihood calculation in this domain neglecting the insignificant elements in the covariance matrix would yield an accurate result and also be computationally efficient. We will present the results corresponding to such an approximate multiscale test in the next section.

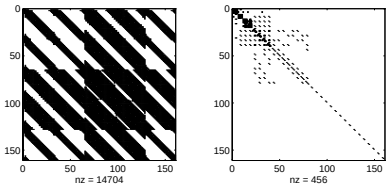

Figure 4: Sparsity patterns of the data model covariance matrix. Left: before the multiscale transform. Right: after the multiscale transform.

6. EXPERIMENTAL RESULTS

We now use our method to discriminate between two natural terrain types, grass and forest, whose SAR images are shown in Figure 1. Based on the estimated correlation structure of these textures, we have decided to model the magnitude of the grass texture by a fractal field with a spectral parameter $\gamma = 1.5$, and the magnitude of the forest texture with $\gamma = 2.5$. Note that the value of γ we have chosen for grass is outside the range of values implied by $0 < H < 1$. This is due to the lack of correlation in the grass texture. Figure 5 shows the spatial correlation structure of the two natural textures estimated from despeckled images. These are in agreement with the parametric fractal models we have chosen to represent them.

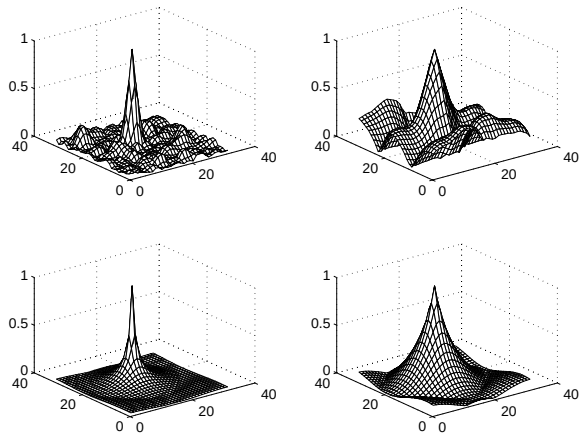

Figure 5: Spatial correlation structures. Top left: grass. Top right: forest. Bottom left: fractal field $\gamma = 1.5$. Bottom right: fractal field $\gamma = 2.5$.

We now use the full-covariance test in (7) and an approximate multiscale test based on (9) to discriminate between 256 grass and forest fields. Our likelihood-based discriminators use a pre-computed, parametric model covariance matrix for each hypothesis. In our multiscale discriminator, we will be using just the diagonal elements of the multiscale data model covariance matrix for an approximate calculation of the likelihoods.

We obtain SAR returns corresponding to the fields by using a discrete spotlight-mode SAR observation model based on system parameters given in [9]. We contaminate the observations so that the SNR is 5 dB, and use only 15% of the data collected from the full aperture. We normalize the energy of the data corresponding to the two hypotheses so that discrimination is done based on textural differences rather than on energy differences. For comparison we also apply two conventional methods [3] for texture discrimination based on fractal dimension. These methods work in the reconstructed image domain. The first method uses the relationship in (4) to do a linear regression on the logarithm of the observed PSD as a function of frequency to determine the fractal dimension. The second conventional method (variance scaling method) estimates the fractal dimension with a logarithmic least squares technique based on the relationship in (5) relating the expected value of the mean-square deviation to displacements.

The receiver operating characteristic (ROC) curves of the approximate multiscale test and that of the full-covariance test along with those of the conventional methods applied to the same data are shown in the left half of Figure 6. The performance of the approximate multiscale test is close to the full-covariance test, although it is computationally much more efficient. The conventional tests perform poorly as compared to the likelihood-based discriminators. We have used only 15% of the data collected from a full aperture for all methods here. While keeping the same, reduced amount of data for the likelihood-based discriminators, we now test the performance of the conventional methods with full-aperture data. The ROCs for this case are illustrated in the right half of Figure 6. This figure shows the likelihood-based discriminators achieve the performance of the conventional methods using much less data than they do.

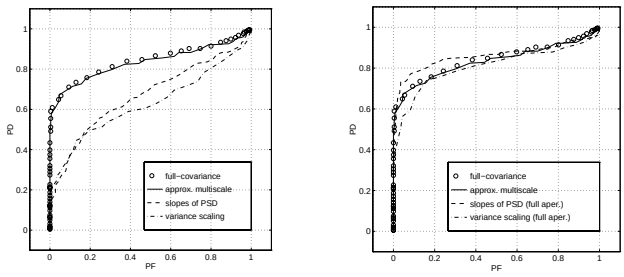

Figure 6: ROCs of proposed and conventional methods (SNR=5dB). Left: all methods using 15% of full-aperture data. Right: conventional methods using full-aperture data

The diagonal approximation of the multiscale data covariance matrix suggests implementing a sequential discriminator. Due to the decorrelated structure inherent in this approximation, the likelihood can be updated after the reception of each data portion, without the need to recalculate the whole likelihood again. This incremental computation could be used to make a decision before having to wait for all the data. Sequential processing of SAR data has also been proposed in [10] for rapid detection. We now show the sequential

calculation of the likelihoods using our approximate multiscale discriminator. As we collect data from a scene, we compute the difference in the approximate multiscale likelihoods, $\hat{L}_{ms}(\text{forest}) - \hat{L}_{ms}(\text{grass})$, and update this value at the reception of every new data portion. Figure 7 shows this computation for SAR returns (SNR=5 dB) from two scenes. The horizontal axis shows the amount of data collected. For the solid curve the data comes from a forest field, and as we collect more data $\hat{L}_{ms}(\text{forest}) - \hat{L}_{ms}(\text{grass})$ becomes larger. For the dashed curve the underlying field is actually grass, and the likelihood difference becomes more negative with data collection, making a correct decision easier. However, for any data set, we can also make an early decision by setting two threshold curves and declaring the sample to be forest if the likelihood difference exceeds the top threshold, and to be grass if it goes below the bottom threshold before all the data are collected. If the threshold is exceeded, this means the data at hand carries characteristic features of one of the hypothesis as opposed to the other, and there is no need to collect all the data. If the threshold is not exceeded at a certain time however, this would mean we need more data for a decision.

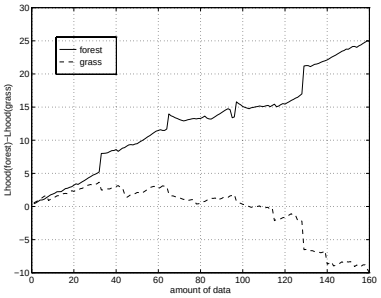

Figure 7: Sequential likelihood test.

7. CONCLUSION

We have developed an approach for discrimination of natural terrain types from noisy and limited SAR returns. Our approach works in the multiscale range profile data domain and is computationally efficient. Furthermore with particular approximations it can be implemented as a sequential test. This method can be a promising alternative to existing methods used for fast prescreening purposes in the process of SAR data collection.

We are currently investigating other rational ways of constructing a likelihood function and approximating the range profile magnitude data covariance matrices in order to improve the performance of our discriminator. We are also interested in considering non-homogeneous textural structures in our framework, which is motivated by problems like target detection and discrimination.

8. REFERENCES

[1] M. C. Burl, G. Owirka, and L. M. Novak, "Texture discrimination in synthetic aperture radar imagery," *Proceedings of the Twenty-Third Asilomar Conference on Signals, Systems and Computers,* pp. 399-404, Nov. 1989.

[2] W. W. Irving, L. M. Novak, and A. S. Willsky, "A multiresolution approach to discrimination in SAR imagery," *IEEE Transactions on Aerospace and Electronic Systems,* vol. 33, pp. 1157-1169, Oct. 1997.

[3] A. P. Pentland, "Fractal-based description of natural scenes," *IEEE Trans. Pattern Anal. Machine Intell.,* vol. PAMI-6, pp. 661-674, Nov. 1984.

[4] C. V. Stewart, B. Moghaddam, K. J. Hintz, and L. M. Novak, "Fractional Brownian Motion Models for Synthetic Aperture Radar Imagery Scene Segmentation," *Proc. IEEE,* vol. 81, pp. 1511-1522, Oct. 1993.

[5] M. Bhatia, W. C. Karl, and A. S. Willsky, "Wavelet-based multiscale stochastic models for efficient tomographic discrimination of fractal fields," *Proceedings of the 1994 IEEE International Conference on Image Processing,* pp. 135-139, Nov. 1994.

[6] D. C. Munson Jr., J. D. O'Brien, and W. K. Jenkins, "A tomographic formulation of spotlight-mode synthetic aperture radar," *Proc. IEEE,* vol. 71, pp. 917-925, Aug. 1983.

[7] M. F. Barnsley, R. L. Devaney, B. B. Mandelbrot, H.-O. Peitgen, D. Saupe, and R. F. Voss, *The Science of Fractal Images,* Springer-Verlag, 1988.

[8] P. Flandrin, "On the spectrum of fractional Brownian motions," *IEEE Trans. Informat. Theory,* vol. 35, pp. 197-199, Jan. 1989

[9] M. Çetin and W. C. Karl, "A statistical tomographic approach to synthetic aperture radar image reconstruction," *Proceedings of the 1997 IEEE International Conference on Image Processing,* pp. 845-848, Oct. 1997.

[10] N. S. Subotic and B. J. Thelen, "Sequential processing of SAR phase history data for rapid detection," *Proceedings of the 1995 IEEE International Conference on Image Processing,* pp. 144-146, Oct. 1995.